Article

Pentacene Disproportionation during Sublimation for Field-Effect Transistors

Luke B. Roberson, Janusz Kowalik, Laren M. Tolbert, Christian Kloc,
Roswitha Zeis, Xiaoliu Chi, Richard Fleming, and Charles Wilkins

J. Am. Chem. Soc., **2005**, 127 (9), 3069-3075• DOI: 10.1021/ja044586r • Publication Date (Web): 10 February 2005

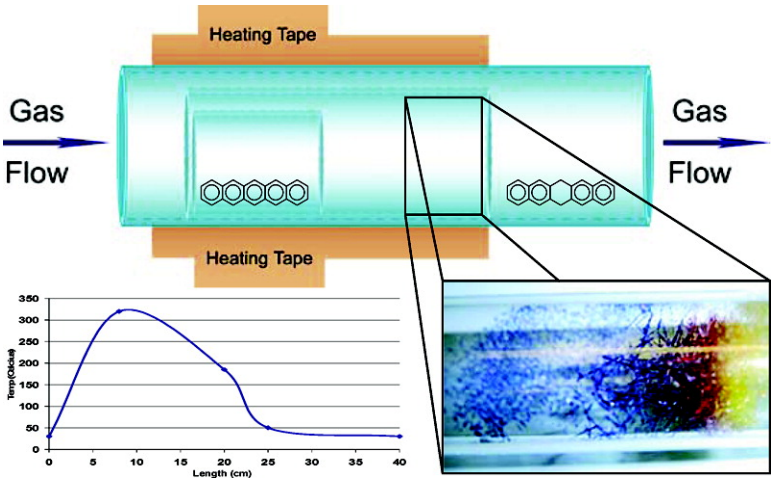

More About This Article

Additional resources and features associated with this article are available within the HTML version:

- Supporting Information
- Links to the 14 articles that cite this article, as of the time of this article download
- Access to high resolution figures
- Links to articles and content related to this article
- Copyright permission to reproduce figures and/or text from this article

View the Full Text HTML

J|A|C|S
ARTICLES
Published on Web 02/10/2005

Pentacene Disproportionation during Sublimation for Field-Effect Transistors

Luke B. Roberson,[†] Janusz Kowalik,[†] Laren M. Tolbert,*[,†] Christian Kloc,*[,‡] Roswitha Zeis,[‡] Xiaoliu Chi,[‡] Richard Fleming,[§] and Charles Wilkins[§]

Contribution from the School of Chemistry and Biochemistry, Georgia Institute of Technology, Atlanta, Georgia 30332, Bell Laboratories, Lucent Technologies, Murray Hill, New Jersey 07174, and Department of Chemistry and Biochemistry, University of Arkansas, Fayetteville, Arkansas 72701

Received September 7, 2004; E-mail: laren.tolbert@chemistry.gatech.edu

Abstract: At moderate temperatures in flowing gas, pentacene undergoes a disproportionation reaction to produce 6,13-dihydropentacene (**DHP**) and a series of polycondensed aromatic hydrocarbons, including the previously unknown peripentacene (**PP**). The process requires activation by heating to 320 °C and is possibly catalyzed by impurities such as **DHP**, 6,13-pentacenequinone (**PQ**), Al, or Fe found in the starting materials. These impurities also result in a decrease in the intrinsic field-effect mobility (FEM) of pentacene crystals. Subsequent purifications remove such impurities, thus inhibiting the formation of the disproportionation products and increasing the FEM of pentacene (2.2 cm^2/Vs). These results clarify the importance of purification of semiconductive materials for measurements of intrinsic mobility and optimal device performance.

Introduction

Pentacene has become the gold standard of materials used in applications such as organic field-effect transistors (OFETs)[1−3] and inorganic−organic hybrid solar cells.[4] Not only does it have one of the highest charge carrier mobilities among organic materials,[5] but it also lends itself to ready purification through vacuum deposition techniques. The mechanism and efficiency of charge transport in organic conjugated semiconductors are known to depend on the purity and frequency of defects along the conjugated backbone.[6] Thus, highly pure, crystalline material is a prerequisite for optimal device performance to ensure that the performance parameters are due to the inherent properties of the material. Commercially available pentacene contains nonnegligible amounts of 6,13-dihydropentacene (**DHP**), 6,13-pentacenequinone (**PQ**), aluminum, and iron, necessitating careful purification, generally by sublimation. We now report that **DHP** is a byproduct of the sublimation itself, which produces other disproportionation byproducts as well, including the hitherto unknown peripentacene. Finally, by careful attention to purification, we are now able to report recent results on OFET properties of highly purified pentacene.

Laudise et al.[7] built a horizontal physical vapor phase reactor to purify and grow crystals for a variety of polyaromatic hydrocarbons under atmospheric conditions. Vapor phase grown pentacene crystals were previously shown to have different polymorphs and higher charge carrier mobility than solution grown crystals.[6,8] More recently, Mattheus et al. have shown that pentacene grown using this method produces different polymorphs within the pentacene crystal structure,[9] which may affect charge carrier mobility. The deposition of pentacene and other polyacenes for device manufacture at atmospheric conditions will be the focus of later reports. However, apparently unique to pentacene is the observation that crystal growth under these conditions leads to hydrogen transfer between pentacene molecules to form **DHP**, and large unsaturated aromatic molecules such as peripentacene, in addition to ultrapure pentacene. We now report details of the formation of these byproducts and provide a proposed mechanism for their formation.

Experimental Procedures

Materials. Pentacene was purchased from Aldrich and TCI America. Perdeuterated pentacene (pentacene-d_{14}; D, 98%) was purchased from Icon Isotopes. Ultrahigh purity (UHP) grade argon (99.97% pure, 4 ppm O_2, 1 ppm total hydrogen content (THC)), Mega BIP grade argon (99.9999% pure, ≤0.2 ppm O_2, ≤0.1 ppm THC), and a mixture of 10% hydrogen in nitrogen were purchased from Air Products. All other materials were purchased from Aldrich and used without further purification.

[†] Georgia Institute of Technology.
[‡] Lucent Technologies.
[§] University of Arkansas.

(1) Kato, Y.; Iba, S.; Teramoto, R.; Sekitani, T.; Someya, T.; Kawaguchi, H.; Sakurai, T. *Appl. Phys. Lett.* **2004**, *84*, 3789−3791.
(2) Minari, T.; Nemoto, T.; Isoda, S. *J. Appl. Phys.* **2004**, *96*, 769−772.
(3) For recent reviews, see (a) Ling, M. M.; Bao, Z. *Chem. Mater.* **2004**, *16*, 4824−4840. (b) Sun, Y.; Liu, Y.; Zhu, D. *J. Mater. Chem.* **2005**, *15*, 53−65.
(4) Senadeera, G. K. R.; Jayaweera, P. V. V.; Perera, V. P. S.; Tennakone, K. *Solar Energy Mater. Solar Cells* **2002**, *73*, 103−108.
(5) Shtein, M.; Mapel, J.; Benziger, J. B.; Forrest, S. R. *Appl. Phys. Lett.* **2002**, *81*, 268−270.
(6) Garnier, F. *Chem. Phys.* **1998**, *227*, 253−262.
(7) Laudise, R. A.; Kloc, C.; Simpkins, P. G.; Siegrist, T. *J. Cryst. Growth* **1998**, *187*, 449−454.
(8) Mattheus, C. C.; Dros, A. B.; Baas, J.; Oostergetel, G. T.; Meetsma, A.; de Boer, J. L.; Palstra, T. T. M. *Synth. Metals* **2003**, *138*, 475−481.
(9) Mattheus, C. C.; de Wijs, G. A.; de Groot, R. A.; Palstra, T. T. M. *J. Am. Chem. Soc.* **2003**, *125*, 6323−6330.

Horizontal Vapor Phase Deposition (HVPD) Furnace. The furnace used for purification and crystal growth of the polyacenes was fabricated with borosilicate glass and was slightly modified from that previously described.[7] The furnace was heated using an Omega heating tape (FGH051-100). Temperature profiles were measured with an Omega digital thermometer (HH12) with two thermocouples. Gas inlet valves were constructed using 24/40 borosilicate glass joints with Tygon tubing or with metal connectors and PTFE tubing. Gas flow rates were varied between 10 and 70 mL/min, with an optimal flow of 30 mL/min.

Characterization. Elemental analyses were performed by Atlantic Microlabs, Inc. using a Perkin-Elmer Series II CHN analyzer 2400. ^{1}H NMR spectra were acquired in deuterated solvents using a 300 MHz Varian Gemini NMR spectrometer. FTIR samples were pressed in dried KBr, and spectra were taken using a Nicolet 520 spectrometer. A Siemens SMART CCD X-ray diffractometer was used for X-ray analysis of single crystals. Solid-state mass spectrometry analyses were performed in both EI (70 and 20 eV) and CI (isobutene) modes on a VG Instruments 70SE. Fourier transform mass spectrometry (FTMS) was performed at the University of Arkansas using a 9.4 T FTMS instrument (IonSpec, Lake Forest, CA). FTMS spectra were obtained by using direct laser desorption using a Nd:YAG laser (New Wave, Sunnyvale, CA) operating at 355 nm. Samples were dissolved in toluene and deposited on a stainless steel target, and the toluene evaporated to form the laser desorption sample. UV−vis spectroscopy was performed on a Perkin-Elmer Lambda 19 UV−vis−NIR spectrometer. High-pressure liquid chromatography (HPLC) was performed using a ChromegaBond C18 reverse-phase column (25 cm × 4.0 mm, 5 μm particle diameter) at 40 °C and 1.0 mL/min flow rate in a 75:25 or 70:30 vol/vol HPLC grade acetonitrile/water mobile phase on a Shimadzu VP series chromatograph equipped with refractive index and UV−vis detectors (210 nm). HPLC-EIMS was performed on a HP 1050 series chromatography using the same column and conditions. Attached to the HPLC was a HP59980B particle beam/LCMS interface equipped with a HP 5989B electron−ionization mass spectrometer (70 eV). Concentrations of all HPLC samples were 1.0 mg/mL dissolved in mobile phase. X-ray photoelectron spectroscopy (XPS) was used for comparison of elemental composition. All angle-resolved spectra were collected using a Physical Electronics (PHI) 1600 XPS system equipped with an AlKα X-ray source. The chamber base pressure during all XPS analyses was at or below 5×10^{-9} Torr. Flame atomic absorption spectroscopy (AAS) was performed by Galbraith Laboratories, Inc. of Knoxville, TN.

Sublimation. Pentacene (30−100 mg, Aldrich or TCI) was placed in the source tube, the source tube was placed inside the deposition tube, and both were placed inside the reactor tube according to Figure 1. Carrier gas was allowed to fill and purge the reactor tube prior to heating. Heat was applied to the tube following a specific heating profile to maximize crystal growth and control the area in which the material deposited (Figure 1). The temperature was monitored both externally, between the heating tape and the reactor tube, and internally with thermocouples and thermometers. The temperature variation at specific locations was less than 3 °C. Sublimation heating times ranged between 4 and 24 h.

Results

Characterization and Purification of Pentacene. The starting materials were characterized by EI/CI-MS, ^{1}H NMR, FTIR, and XPS, which showed no evidence of oxygen or aliphatic hydrogens with pentacene obtained from any of the suppliers. However, HPLC/UV−vis spectroscopy and electron impact mass spectrometry (EIMS) indicated a small concentration of **DHP** and other impurities at very low concentrations.

While obtaining optimal sublimation conditions for pentacene, a distinct deposition profile was observed at sublimation temperatures exceeding 320 °C (Figure 1). This sublimation

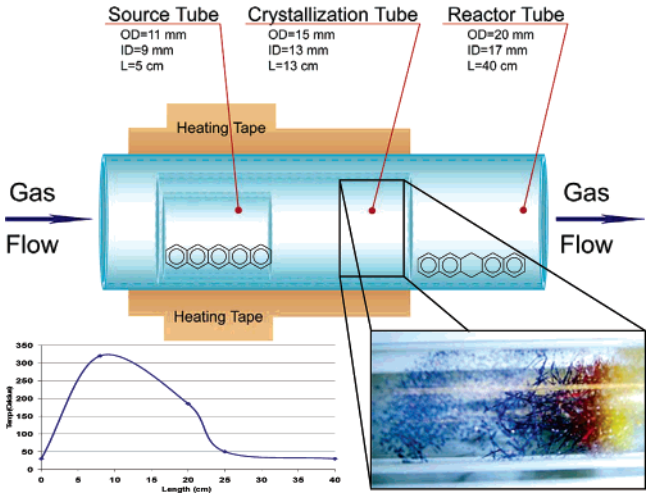

Figure 1. Diagram of the horizontal physical vapor deposition (HPVD) chamber used for the sublimation and crystal growth of pentacene. The temperature profile shows the temperatures measured for the sublimation process along with an aid-to-the-eye line. The inset depicts the overlapping crystal boundaries of purple pentacene crystals with the red and yellow 2:1 **DHP**/pentacene cocrystals.

gave rise to large plate and needle-shaped, dark blue-violet colored crystals as large as the diameter of the deposition tube, as well as a yellow powder, yellow and red needle-shaped crystals, and a brittle black residue with a metallic luster. The purification was strongly dependent upon the operating conditions of the furnace. As the material sublimed, it was transported by the carrier gas to the crystal growth zone, where dark blue crystals, identified as pentacene, appeared. In addition, yellow and red, needle-shaped crystals, previously identified as a 2:1 **DHP**/pentacene cocrystal,[10] were deposited in the impurity deposition zone concomitantly with **DHP**,[11] 6-pentacenone, and **PQ**. The color difference between yellow and red cocrystals was associated with a slight difference in impurity concentration within the crystal. Pentacene impurities led to the red color, while **DHP** produced yellow crystals. Removal of impurities led to colorless crystals. Independent of the amount of starting material used, the ratio of residue to pentacene to **DHP** was nearly always 25:50:25% at source temperatures above 350 °C. After purification, a black, glassy residue remained in the source zone. However, sublimations over extended periods of time at source temperatures below 300 °C resulted in no observable formation of any residue or byproducts.

The carrier gas played little apparent role in the distribution of byproducts formed during sublimation. Using any of the three carrier gases, the distribution pattern of **DHP** and cocrystal remained relatively unchanged. The introduction of 10% hydrogen in nitrogen at these temperatures also did not affect the yield of hydrogenated byproducts versus UHP or Mega BIP grade argon. Oxygenated byproducts (6-pentacenone and **PQ**) were observed when UHP grade argon was employed. Oxygen in excess of 2 ppm resulted in the oxygenated products, whereas with Mega BIP grade argon with oxygen concentrations less than 0.2 ppm we were unable to detect any oxygenated products. Because of the formation of 6-pentacenone, **PQ**, and 6,13-pentacenequinone-d_{12} (observed by EI/CI-MS) using UHP

(10) Mattheus, C. C.; Baas, J.; Meetsma, A.; de Boer, J. L.; Kloc, C.; Siegrist, T.; Palstra, T. T. M. *Acta Crystallogr., Sect. E* **2002**, *E58*, 1229−1231.
(11) Spectral Data: ^{1}H NMR ($CDCl_3$): d 7.78 (t, 8H) 7.42 (dd, J = 6.6 Hz, 4H) 4.25 (s, 4H), and EIMS M^+ = 280 m/z.

Table 1. Elemental Analysis and AAS Data for Pentacene Starting Material and Sublimation Products

element	Aldrich pentacene	purified pentacene	residue	DHP
% C	95.01 (94.96)[a]	94.91 (94.96)	94.15 (96.70)	93.82 (94.29)
% H	5.10 (5.04)	4.96 (5.04)	4.83 (3.30)	5.82 (5.71)
% O	0.00	0.00	0.00	
% N	0.00	0.00	0.00	0.00
% Fe	114 ppm		719 ppm	
% Al	593 ppm		1.76	

[a] Theoretical values in parentheses, including peripentacene for the residue.

argon, the purification process was examined to determine the source of oxygen. Ridox and Drierite ($CaSO_4$) columns installed to remove oxygen and water from the carrier gas failed to hinder the formation of **PQ**. Experiments using Mega BIP argon or a vacuum-sealed ampule at 10^{-3} Torr failed to produce the corresponding quinone yet still produced **DHP** and cocrystal with no change in percent yield.

To prove that hydrogen was not infiltrating the system adventitiously, 30 mg of either Aldrich pentacene or purified pentacene was placed into a sealed ampule under vacuum at 10^{-3} Torr. Heating the ampule to 320 °C in a sand bath or in the furnace resulted in the formation of **DHP**, cocrystal, and the black residue in both circumstances. The product ratio remained approximately 25:50:25 **DHP**, purified pentacene, and residue. However, these reactions showed no increase in oxygenated products. Additionally, purification of pentacene-d_{14} (EIMS $M^+ = 292$ *m*/*z*) tested under the same sublimation conditions and using a vacuum-sealed ampule resulted in the formation of 6,13-dihydropentacene-d_{16} (**DHP-*d*$_{16}$**) (EIMS $M^+ = 296$ *m*/*z*), with no incorporation of hydrogen seen with either EI or CIMS under either argon atmospheres, yet using the UHP grade argon resulted in the formation of the perdeuterated oxygenated pentacenes: 6-pentacenone-d_{14} (EIMS $M^+ = 308$ *m*/*z*) and 6,13-pentacenequinone-d_{12} (EIMS $M^+ = 320$ *m*/*z*).

Depending on the operating conditions, it was possible to manipulate the type of the purified pentacene crystals produced. At source temperatures between 265 and 285 °C and deposition temperatures at 165 °C, needle-shaped crystals were produced. Increasing the source temperature to or above 310 °C and deposition temperature to 185 °C resulted in large plates. Elemental analysis of the needle and plate-shaped crystals showed a 100% composition of carbon and hydrogen in a C:H ratio of 18.6 as compared to the theoretical value of 18.7 for pentacene (Table 1). FTIR spectra indicated the presence of only aromatic C−H bonds at 3040 cm^{-1}. Single-crystal X-ray diffraction structures obtained from the needle and plate crystals were essentially identical to the lattice dimensions for vapor-phase grown pentacene previously reported.[8,9,12] Additionally, the lattice dynamic calculations and lattice dimensions match those of Venuit et al.[13] for vapor-phase grown pentacene. Although Mattheus et al. obtained different pentacene polymorphs using this method,[8] we only observed the 14.1 Å polymorph in both needle and plate-shaped crystals.

Identification of Peripentacene (PP). The appearance of the residue within the source tube following the sublimation of pentacene varied based on the source temperatures used during sublimation. At source temperatures between 320 and 375°C, the residue appeared as a black powder; however, at temperatures exceeding 380 °C, the residue melted into a glassy state.

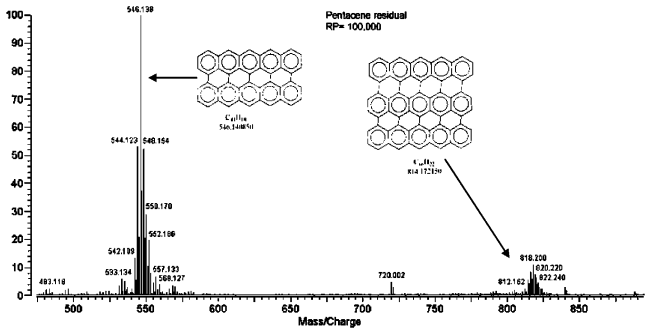

Figure 2. Direct 355 nm laser desorption FTMS of the pentacene residue.

The identity of the residue was established based on the FTMS spectrum shown in Figure 2. As seen in the figure, the mass peak at 546 *m*/*z*, measured with resolving power of 100 000, corresponds within 7 ppm to the composition of the previously unknown peripentacene (**PP**). The distribution pattern of the peaks around 546 *m*/*z* can be explained by the positioning of the two pentacene rings relative to one another. A slight offset in ring fusion or an unfused position would result in an increase in molecular mass by 2, 4, or 6. The peak with *m*/*z* 818 corresponds to trisperipentacene with two unfused positions (i.e., $C_{66}H_{26}^+$).

The initial FTIR spectrum of the residue exhibited both aromatic and aliphatic C−H stretching.[14] However, further analysis revealed the presence of **DHP** in the residue, requiring further purification. Electrical conductivity measurements performed using a Quantum Design Physical Properties Measurement System (PPMS) run with Lab View showed the material to be more conductive than pentacene, with a linear I−V dependence similar to graphite. Single-crystal X-ray diffraction could not be obtained because of the high reflectivity of the glassy samples. Powder X-ray diffraction revealed a *d* spacing of 7.43 Å, almost half of the 14−15 Å *d* spacing of the different pentacene polymorphs[9] and twice that of the 3−4 Å *d* spacing of graphite and single-walled carbon nanotubes.[15]

Elemental Analysis and FTIR Trends. Elemental analyses were performed to illustrate a direct trend in hydrogen content between sublimation products. The results showed a 5% decrease in hydrogen content between the Aldrich starting material and the black, glassy residue containing **PP** (Table 1). In addition, the **DHP** and the cocrystal showed an increase in hydrogen when compared to the starting material. The differences associated with the **DHP** and cocrystal elemental analysis are presumably due to the difficulty in separating the overlapping of byproducts within the impurity deposition zone. The elemental analysis also showed a slight oxygen content within the **DHP** formed under the UHP argon atmosphere.

The infrared spectrum of the Aldrich starting material duplicated previous results and did not show aliphatic C−H bond stretching.[14,16] The presence of the large aliphatic C−H stretch observed in the **DHP** and cocrystal spectra demonstrate a trend in the loss of aromaticity from the starting material.

(12) Anthony, J. E.; Eaton, D. L.; Parkin, S. R. *Org. Lett.* **2002**, *4*, 15−18.
(13) Venuti, E.; Della Valle, R. G.; Brillante, A.; Masino, M.; Girlando, A. *J. Am. Chem. Soc.* **2002**, *I*, 2128−2129.
(14) Roberson, L.; Kowalik, J.; Tolbert, L.; Kloc, C. *Polym. Mater. Sci. Eng.* **2003**, *89*, 410−411.
(15) Yoshizawa, K.; Yumura, T.; Yamabe, T.; Bandow, S. *J. Am. Chem. Soc.* **2000**, *122*, 11871−11875.
(16) Supplier provided data (www.aldrich.com).

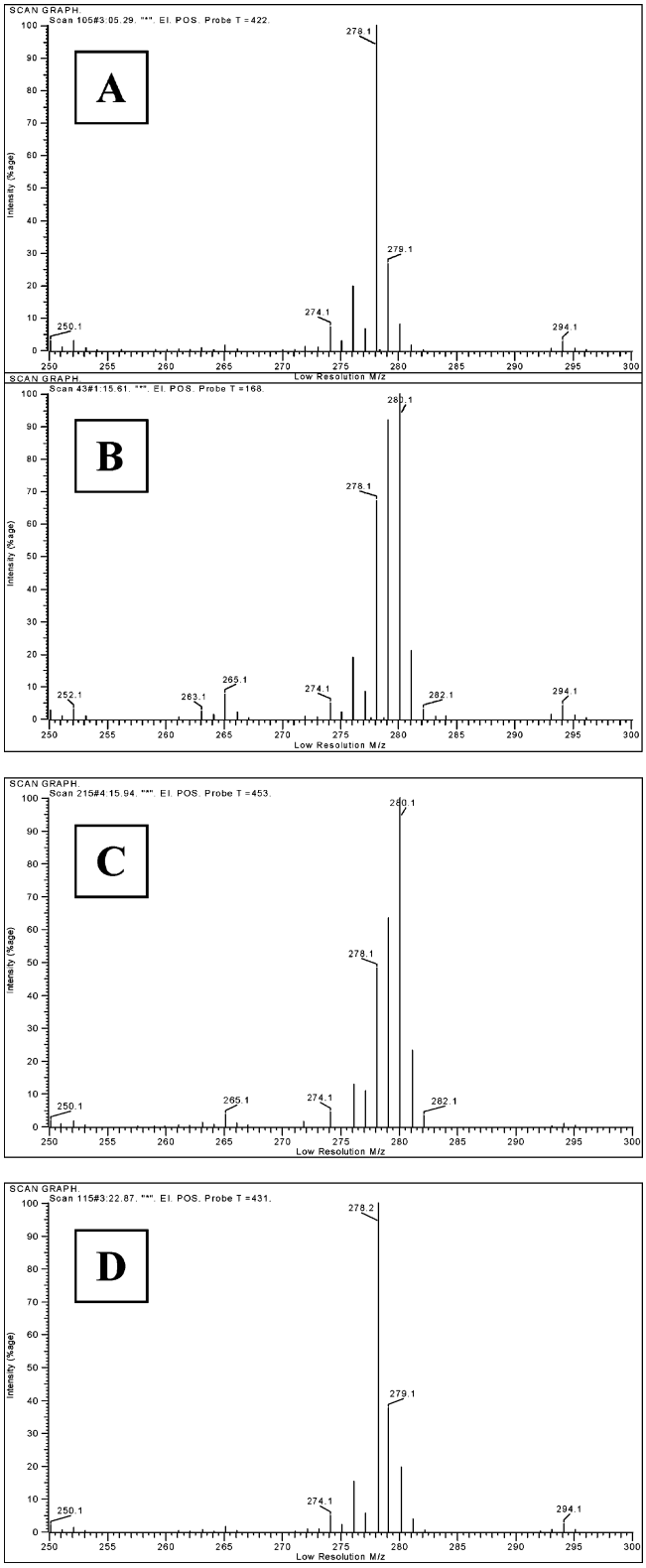

Figure 3. Solid-state EIMS of (A) Aldrich pentacene, (B) **DHP**, (C) cocrystal, and (D) purified pentacene from 250 to 300 *m*/*z*.

The FTIR spectrum of the unpurified residue contained C−H absorptions similar to those for pentacene and **DHP**; however, the residue also contained additional vibrations above 3000 and at 2925 cm^{-1}.

Solubility and Comparison of Absorption Spectra. A 5.6 mg sample of glassy residue prepared using Mega BIP argon as the carrier gas was ground with a glass rod and dissolved in 2 mL of 1,2,4-trichlorobenzene (**TCB**), resulting in a black solution. UV−vis absorption spectroscopy of this solution revealed an unstructured absorption with significant oscillator strength at 800 nm. However, 4.8 mg of Aldrich pentacene treated similarly at room temperature did not dissolve but rather remained at the surface of the **TCB**. Heating the mixture to 60 °C resulted in a purple solution. Upon cooling, the solution remained a light purple color with considerable reprecipitation. After 30 min, the color disappeared to leave crystals floating on the surface, and after 12 h, the supernatant turned yellow.

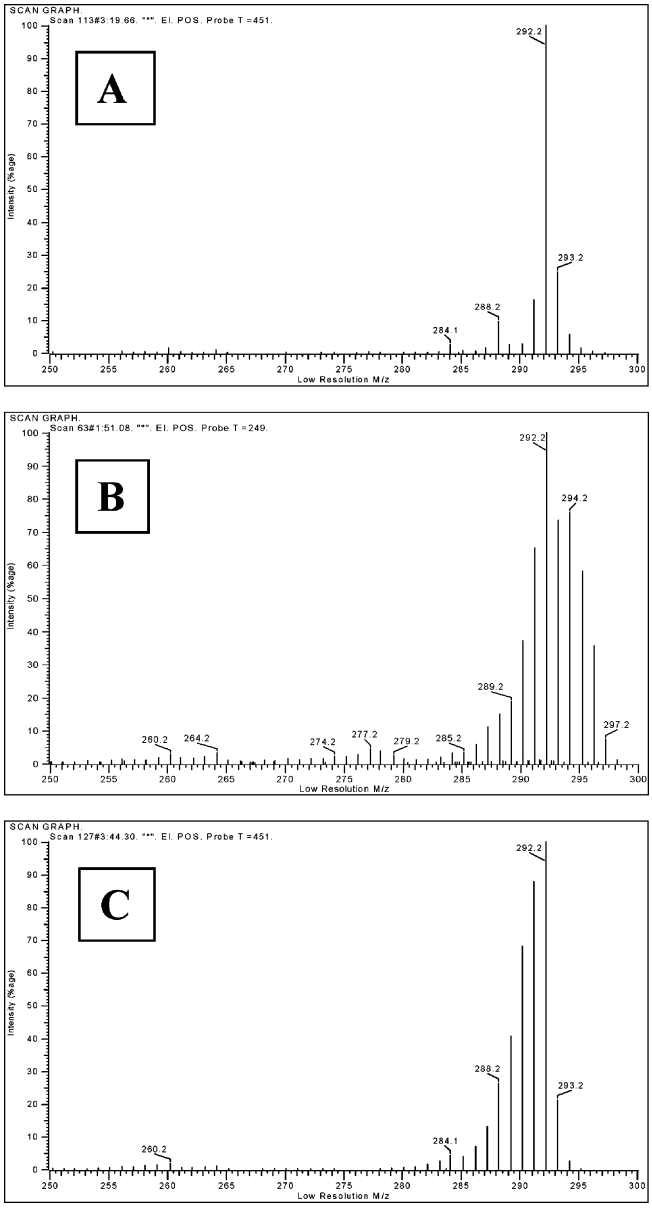

Figure 4. Solid-state EIMS of (A) ICON pentacene, (B) **DHP-d_{16}**, and (C) purified pentacene-d_{14}.

Chromatography. High-pressure liquid chromatography (HPLC) was carried out based on the work of Baweja, who separated hydrogen and deuterium analogues of polyaromatic hydrocarbons (PAH) using various mixtures of ACN/H_2O mobile phase and a C18 reverse phase column.[17,18] In addition

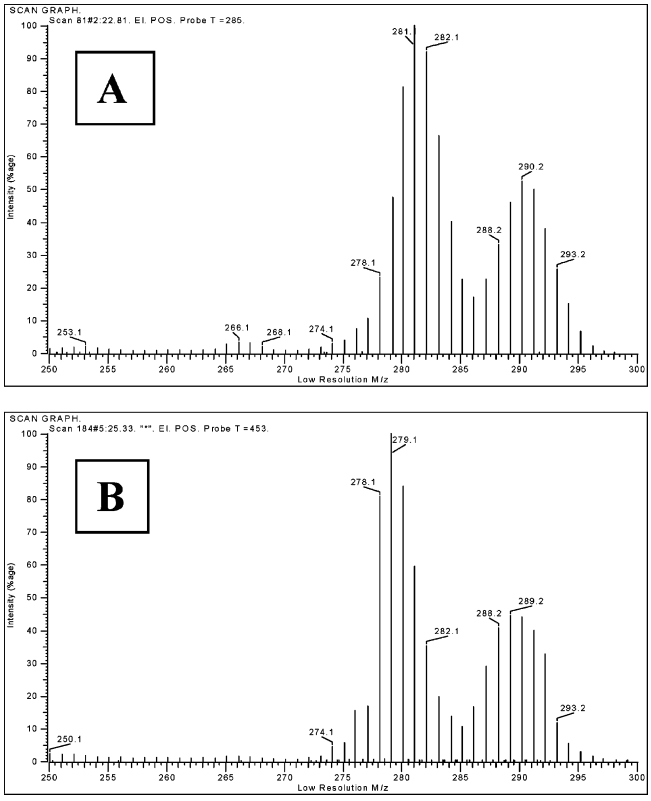

Figure 5. Solid-state EIMS of (A) mixed H/D 6,13-dihydropentacenes and (B) mixed H/D pentacenes.

to the HPLC−RID, a UV−vis and a particle beam interface EIMS detector were used to accurately identify the separated compounds. The separation of peaks varied as a function of mobile phase concentration and aromatic hydrocarbon; however, the separation of hydrogen and deuterium analogues was typically greater than 1 mL. We were able to reproduce his results with a small difference in retention times between standard PAHs such as benzene and anthracene. Using this separation technique, we were able to separate and identify hydrogen and deuterium analogues of the pentacene products. The solubility of pentacene within this mobile phase was very poor, yet certain impurities were identified via EIMS such as **DHP** and **PQ**. As expected, **DHP** (12.3 mL) eluted more rapidly than pentacene (15.0 mL). This was the same for the deuterium analogues **DHP-*d*$_{16}$** and pentacene-*d*$_{14}$, which eluted at 11.0 and 14.3 mL, respectively. Similarly to Baweja, we observed that the deuterium analogue eluted before the hydrogen analogue in both cases.

EIMS Comparison. The solid-state EIMS of the Aldrich pentacene, **DHP**, cocrystal, and purified pentacene samples are shown in Figure 3. The Aldrich pentacene and purified pentacene spectra were identical, with M^+ peaks at 278 *m*/*z* at column temperatures at 452 °C. The **DHP**, M^+ peak at 280 *m*/*z*, came off at a column temperature at 265 °C. The FTMS of the residue was described previously; however, EIMS of the residue in **TCB** resulted in a spectrum containing an M^+ peak at 556 *m*/*z* at a column temperature of 453 °C; showing the presence of a single-bonded bipentacene, as well as the observed **DHP** and pentacene fractions isolated at their respective column

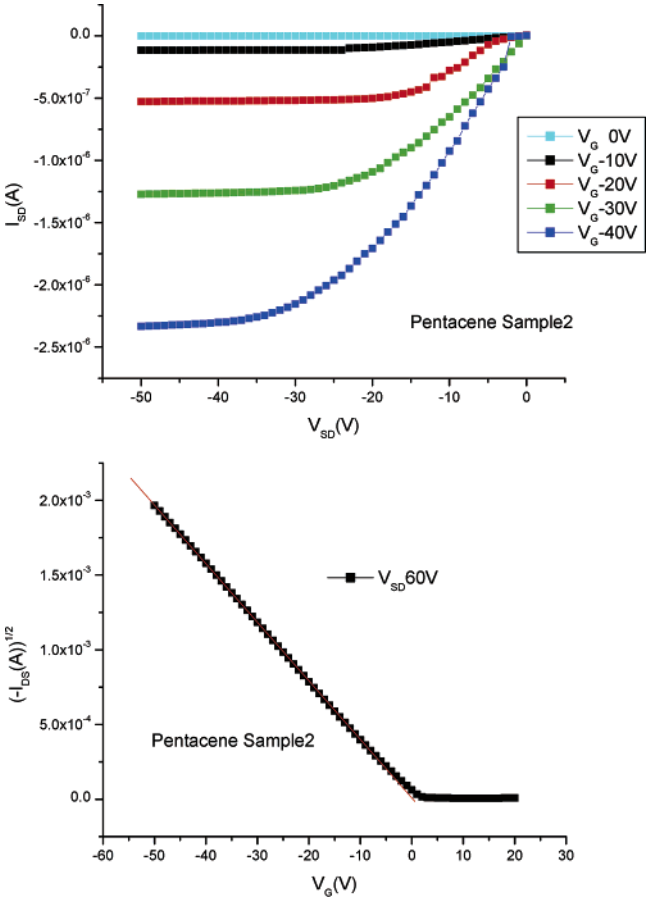

Figure 6. *I*−*V* curves for pentacene single-crystal field-effect transistors: (A) source-drain current vs source-drain voltage for various gate voltages and (B) source-drain current vs gate voltage for the saturation region at $V_{SD} = -60$ V leading to a calculated hole mobility of 2.2 cm^2/V·s.

temperatures. Perdeuterated samples were also tested for comparison (Figure 4). The observed fractionation patterns between hydrogenated and deuterated products were nearly identical.

Crossover Experiments. To determine the extent of intramolecular hydrogen transfer reactions, 17.9 mg of Aldrich pentacene was mixed with 12.5 mg of pentacene-*d*$_{14}$ (ICON) and heated in the HPVD chamber at a source temperature of 380 °C for 4 h. The mixed reaction products were isolated and collected. EIMS of the mixed dihydropentacene (Figure 5A) and mixed pentacene (Figure 5B) samples were analyzed. Upon comparison with the purely hydrogenated and deuterated 6,13-dihydropentacenes and pentacenes, there was a very good mixed distribution of hydrogen and deuterium products within the mixed samples. Overlap of the original respective hydrogenated and deuterated EIMS spectra would not have resulted in the spectrum obtained for the mixed samples. HPLC of the mixed dihydropentacene was run against the **DHP** and **DHP-*d*$_{16}$**. The result was a broad chromatogram with four local maxima between the **DHP** maximum at 13.5 min and the **DHP-*d*$_{16}$** maximum at 12.5 min. The local maxima are attributed to the mixed and original samples.

Field-Effect Measurements. Taking into account the previously described formation of pentacenequinones, hydrogenated pentacene, and peripentacenes, the following procedure was used for preparation of ultrapure single crystals, and field-effect

(17) Baweja, R. *Anal. Chim. Acta* **1987**, *192*, 345−348.
(18) Kline, W. F.; Wise, S. A.; May, W. E. *J. Liq. Chromatogr.* **1985**, *8*, 223−237.

Table 2. Ab Initio and AM1 Heats of Formation and Reaction for the Proposed Zipper-Effect for the Formation of Peripentacene and 6,13-Dihydropentacene from Pentacene

Hydrocarbon	Structure	ΔH_f (a.u.)	ΔH_r (kcal/mol)	ΔH_f (kcal/mol)	ΔH_r (kcal/mol)
		ab initio		AM1	
Pentacene	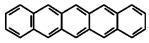	-836.5685		111.9	
Dihydropentacene	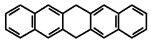	-837.7675		75.8	-36.1
Bipentacene	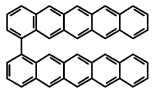	-1671.9848	-29.5	231.0	-28.8
Dehydrobipentacene	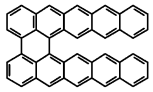	-1670.8144	-47.4	241.3	-54.6
Bisdehydrobipentacene	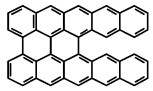	-1669.6756	-85.2	242.6	-89.4
Trisdehydrobipentacene		-1668.5402	-125.1	242.3	-125.8
Peripentacene (**PP**)		-1667.4238	-177.0	231.2	-172.9

transistors were built with these crystals. First, commercial pentacene was sublimed in a 30 mL/min flow of argon at 200−320 °C temperature gradient. The pentacene crystals were accompanied by a black residue in the evaporation source and a violet-blue deposit in the low temperature region. Pentacene crystals separated from residues were used for subsequent crystal growth in a sealed ampule. The absence of inert gas provided for sublimation at a slightly lower temperature thereby producing thicker crystals.

On the large flat (001) surface were painted carbon source and drain electrodes and thermally evaporated perylene, followed by vacuum evaporated silver gate electrodes. The transistor was wired, and the electrical characteristics were measured using a probe station connected to a HP semiconductor parameter analyzer 4145B. The OFET I−V characteristics are presented in Figure 6. From these data a hole mobility was calculated to be 2.2 cm^2/Vs.

Discussion

Studies of the thermal reactivity of polyaromatic hydrocarbons have been reported since the 1960s, for which the carbonization of PAH via hydrogen transfer is monitored by differential thermal analysis.[19] Additionally, high mechanical pressures have been shown to produce graphitic species and dihydrogenated and tetrahydrogenated byproducts from polyacenes via hydrogen transfer.[20] Ab initio (3-21G*) and semiempirical (AM1) calculations for the hydrogenation of pentacene to dihydropentacene and from pentacene to **PP** were performed to rationalize the observed hydrogen transfer (Table 2). These results showed the heat of hydrogenation of pentacene to be 36.1 kcal/mol, while the heat of dehydrogenation of pentacene to 1,1′-bipentacene is 7.3 kcal/mol, providing an overall enthalpy for the reaction of −28.8 kcal/mol. In that regard, it is interesting to consider the individual steps of the zipper reaction that converts 1,1′-bipentacene into **PP**. Of course, the actual mechanism may involve a number of different intermediates with differing fusion points, although initial reaction at C-6 represents a plausible starting point (Figure 7). We would also expect at these temperatures that considerable redistribution among various connectivities would lead to intermediates allowing for final ring fusion. Nevertheless, assuming a symmetrical order of bond formation, we see that each successive bond after the second delivers a greater enthalpy. This observation may represent a general mechanism for graphitization reactions since there is apparently a kinetic driving force for planarization once the aryl−aryl bonds begin to form.

The mechanism of the hydrogen transfer reaction itself is still unclear. Polyacenes are well-known to undergo radical reactions, and the possibility of a catalytic reaction involving the formation of radicals was considered. The source of a radical initiator was explored to determine the initiation step of the mechanism. Flame AAS was used to see if Fe or Al was present in the Aldrich or ICON starting materials. Iron is known to be a catalyst for radical reactions;[21,22] whereas, Al is commonly used as a catalyst in the synthesis of pentacene from **PQ**.[23] AAS

(19) Lewis, I. C.; Edstrom, T. *J. Org. Chem.* **1963**, *28*, 2050−2057.
(20) Field, L. D.; Sternhell, S.; Wilton, H. V. *Tetrahedron* **1997**, *53*, 4051−4062.
(21) Yamamoto, K.; Tanaka, H.; Sakaguchi, M.; Shimada, S. *Polymer* **2003**, *44*, 7661−7669.
(22) O'Reilly, R. K.; Gibson, V. C.; White, A. J. P.; Williams, D. J. *J. Am. Chem. Soc.* **2003**, *125*, 8450−8451.

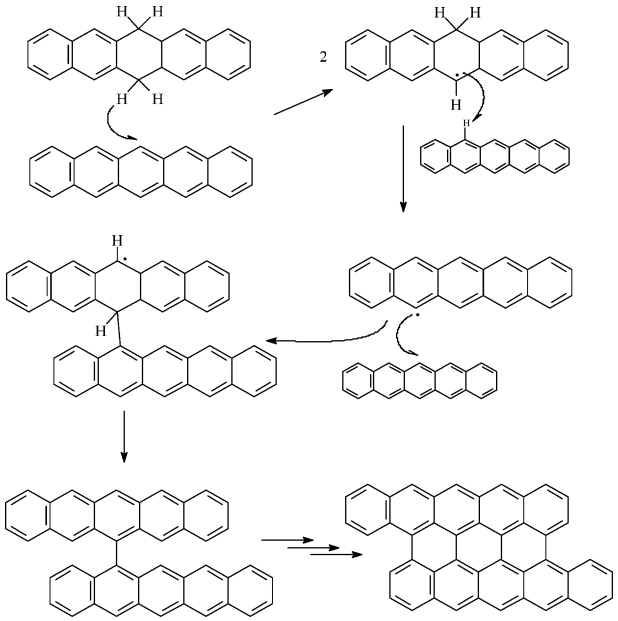

Figure 7. Proposed reaction mechanism for the hydrogen transfer of pentacene during sublimation at 1 atm pressure.

results showed small concentrations of both Fe (114 and 719 ppm) and Al (593 ppm, 1.76%) in the Aldrich and residue samples, respectively. As expected, the concentrations of the metals in the residues were greater than that in the Aldrich material since the metals do not sublime. Rüchardt's hydrogen transfer experiments using 9,10-dihydroanthracene as the radical initiator have led us to believe that small concentrations of **DHP** are acting similarly in our experiments.[24,25] We note that HLPC trace chromatograms showed the presence of small amounts of **DHP** in pentacene, and it is possible that this is an autocatalytic reaction, with **DHP** acting as the radical initiator with the loss of hydrogen at the 6 position at temperatures exceeding 320 °C (Figure 7). This mechanism is consistent with Rüchardt's observations on the hydrogen transfer reduction of styrene.[26,27] We note that the crossover experiments, indicating scrambling of hydrogen and deuterium in the **DHP** products, are permissive of such a mechanism but not exclusive to it. Moreover, the temperature of the transformation is similar to that required under Rüchardt's conditions using dihydroanthracene as the hydrogen donor. Although we see no evidence for this process, it has been suggested that the butterfly photodimer[28] present in some preparations of pentacene could also lead to pentacenyl radicals through bond scission at high temperature, which would obviate the formation of slip isomers of the pentacene dimers and trimers. Conversely, formation of peripentacene and its higher homologues may occur via isomerization of such intermediate slip isomers of bipentacenes formed under these conditions.

Finally, having achieved high-purity pentacene, we were able to perform mobility measurements. Single-crystal field-effect transistors were constructed on single crystals grown using a horizontal vapor phase reactor, producing a hole mobility up to 2.2 cm^2/Vs. This high value was possible to achieve because the two-step crystal growth and purification process was applied. OFETs have been prepared using low-temperature electrodes and dielectric deposition processes, which limited defect formation in the FET channel and in source gate electrode areas.

Conclusion

The preparation and purification of organic materials for electronic devices continues to be a challenge to the field of organic electronics.[29] Even well-characterized materials such as pentacene are capable of significant impurity-forming reactions at relatively low temperatures. Such results serve as a caution to overinterpretation of results based upon materials that may have defects at extremely low concentrations, which nevertheless impact device performance. Fortunately, it is possible to limit the concentration of impurities and defects and produce single-crystal field-effect transistors with relatively high hole mobility. Such careful analysis and purification, when applied to thin film transistors, can improve pentacene thin film field-effect transistors and can be widely applicable into industry scale organic microelectronic devices.

Acknowledgment. We gratefully acknowledge the U.S. Department of Energy (DE-FG02-85ER45194) for their financial support. We thank Drs. Don Vanderveer, Oliver Just, and Jack Eichler for single-crystal X-ray crystallography data and interpretations for all aforementioned crystals. We thank Joe Carlise and Dr. Victor DeJesus of the Georgia Tech Research Institute (GTRI) for training and use of HPLC/UV−vis and HPLC−EIMS. Finally, we thank Dr. Theo Siergist for powder X-ray data and insightful discussions. L.B.R. thanks the Intel Foundation for an Intel Foundation Fellowship Award.

Supporting Information Available: Experimental details. This material is available free of charge via the Internet at http://pubs.acs.org.

JA044586R

(23) Kwant, B. H. *J. Labeled Comp. Radiopharm.* **1978**, *14*, 397−401.
(24) Rüchardt, C.; Gerst, M.; Ebenhoch, J. *Angew. Chem., Int. Ed.* **1997**, *36*, 1406−1430.
(25) Keller, F.; Rüchardt, C. J. *Prakt. Chem./Chem.-Ztg.* **1998,** *340*, 642−648.
(26) Friebolin, H.; Roers, R.; Ebenhoch, J.; Gerst, M.; Rüchardt, C. *Liebigs Ann. Chem.* **1997**, 385−389.
(27) Morgenthaler, J.; Rüchardt, C. *Eur. J. Org. Chem.* **1999**, 2219−2230.
(28) Berg, O.; Chronister, E. L.; Yamashita, T.; Scott, G. W.; Sweet, R. M.; Calabrese, J. *J. Phys. Chem. A* **1999**, *103*, 2451−2459.
(29) For a discussion, see Jurchescu, O. D.; Bass, J.; Palstra, T. T. M. *Appl. Phys. Lett.* **2004**, *84*, 3061−3063.